Non-Fourier Heat Flux Model for the Magnetohydrodynamic Casson Nanofluid Flow Past a Porous Stretching Sheet using the Akbari-Gangi Method

AMINE EL HARFOUF[1,*], RACHID HERBAZI[2,3,4], SANAA HAYANI MOUNIR[1],
HASSANE MES-ADI[5], ABDERRAHIM WAKIF[6]

[1]Multidisciplinary Laboratory of Research and Innovation (LaMRI),
Energy, Materials, Atomic and Information Fusion (EMAFI) Team,
Polydisciplinary Faculty of Khouribga,
Sultan Moulay Slimane University,
MOROCCO

[2]Intelligent Systems and Applications Laboratory (LSIA), EMSI,
Tangier,
MOROCCO

[3]ENSAT, Abdelmalek Essaâdi University,
Tangier,
MOROCCO

[4]ERCMN, FSTT, Abdelmalek Essaâdi University,
Tangier,
MOROCCO

[5]Laboratory of Process Engineering, Computer Science and Mathematics,
National School of Applied Sciences of the Khouribga University of Sultan Moulay Slimane,
MOROCCO

[6]Faculty of Sciences Aïn Chock, Laboratory of Mechanics,
Hassan II University,
Casablanca,
MOROCCO

Corresponding Author

Abstract: - The Casson fluid flow with porous material in magnetohydrodynamics is examined in this work. Additional semi-analytical results are investigated using the Silver-Water nanofluid. The Akbari-Ganji Method (AGM) is used to solve the semi-analytical Cattaneo-Christov heat flux model after taking thermal radiation into account. With the use of appropriate parameters, such as the relaxation time parameter, Prandtl number, radiation parameter, magnetic parameter, and so on, the normalized shear stress at the wall, temperature profile, and rate of heat flux may be examined. This issue has numerous industrial applications and technical procedures, such as the extrusion of rubber sheets and the manufacture of glass fiber. The main physical application is the discovery that a rise in the thermal relaxation parameter and Prandtl number maintains a constant fluid temperature.

Key-Words: - Magnetohydrodynamics; Porous medium; Couple stress; Nanofluid; The Akbari-Ganji Method (AGM); porous stretching sheet.

Received: March 13, 2023. Revised: December 27, 2023. Accepted: February 26, 2024. Published: April 2, 2024.

1 Introduction

Non-Newtonian fluids have drawn a lot of attention because of their wide range of applications, which include cooling engines and extracting crude oil from petroleum products, [1]. Like this, stretching sheet issues are important in the engineering domains. The authors [2], were the first to pioneer the study of laminar flow problems, and researchers later expanded on this work, [3]. In this work, fluid flow occurred because of stretching the sheet. As a result of their work, numerous scholars investigated the problems associated with stretching sheets. Stretching sheet difficulties were studied by [4] and [5]. In addition, in other work [6], using various media. Fluid flow happened in the presence of a porous media. There are numerous industrial uses for this phenomenon. Subsequently, nanofluids are used to solve stretching sheet problems in conjunction with other fluids and boundary conditions. The thermal properties of nanofluids were studied in [7], [8], [9] and some of the magnetorheological properties were also reviewed. In addition to the computational time, the authors [10] and [11] investigated nanofluids with suction and laminar natural convection. Additional instances about nanofluids are enumerated in [12], [13] and [14]. Only the momentum and energy equations with the classical Fourier law are covered by the books. As a result, research is done on the temporal relaxation parameter, [15], [16]. The derivatives of the usual type are transformed into Oldroyd's upper convicted derivative, which is known as the Cattaneo-Christov heat flux and was enhanced by [17].

The current work, which discusses the heat transfer properties of Casson fluid flow through a porous material with radiation, was inspired by previous research. Non-Newtonian fluid behavior is typically described by Casson fluid models. The current work is unusual in that it uses analytical tools to characterize the flow behavior of the Casson fluid and adds nanoparticles to the fluid's surface to increase thermal efficiency. Additionally, the primary methodology describes how to solve the stretching sheet problem analytically using the Appell hypergeometric technique and a time relaxation parameter. The Cattaneo-Christov equation is used in this case to transform ordinary-type derivatives into Oldroyd's upper convicted derivative. then straight integration is used to solve the temperature equation. Industrial, biomedical, and engineering processes are the primary physical components of the present. Refer to the Casson fluid flow research conducted by [18] and [19].

2 Mathematical Formulations

In the current investigation, a non-Newtonian fluid flow with porous media and MHD is analyzed. Silver-water nanofluid is another fluid that is added to the flow. The schematic diagram utilized in this investigation is described in Figure 1 and the amounts of nanofluid are shown in Table 1.

The Maxwell's equation

$$\vec{J} = \mu_m \sigma\left(\vec{q} \times \vec{B}\right) \quad (1)$$

$$\nabla \cdot \vec{B} = 0 \quad (2)$$

$$\nabla \times \vec{B} = \sigma \, \vec{E}_{int} \quad (3)$$

$$\nabla \times \vec{E}_{int} = -\mu_m \frac{\partial \vec{B}}{\partial t} \quad (4)$$

Here $\vec{E}_{int} = \mu_m\left(\vec{q} \times \vec{B}\right)$ stands for the induced electric field, while other terms are defined according to the nomenclature. The Maxwell equations are usually integrated into a single equation called the magnetic induction equation in magneto-convection.

However, the magnetic Rayleigh number $Rm = \mu_m \sigma V d << 1$ can be obtained by applying the constitutive Eq. (1). $Vd << 1$ (here V is Characteristic velocity), and the Lorentz force $\mu_m \left(\vec{J} \times \vec{B}\right)$ for weak conducting fluid can be written as:

$$\mu_m \left(\vec{J} \times \vec{B}\right) = -\mu^2 \sigma {B_0}^2 u.$$

This is known as the Hartmann formulation of the magnetohydrodynamic issue.

Table 1. Thermo-physical properties of water and nano particles.

	ρ $(Kg\,/\,m^3)$	Cp $(J\,/\,Kg.K)$	K $(W\,/\,m.K)$	$\sigma(Sm^{-1})$
Pure water (H_2O)	997.1	4179	0.613	0.05
Silver (Ag)	10,500	235	429	5.97*10^7

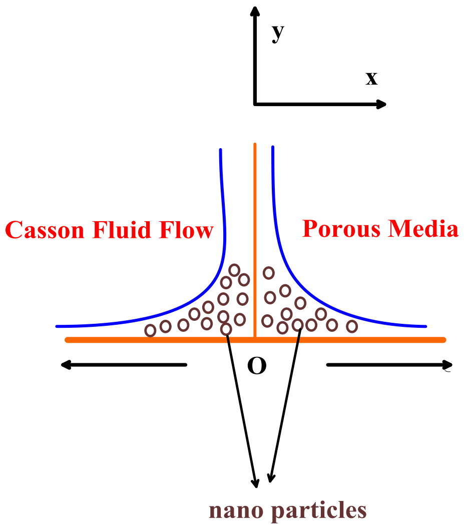

Fig. 1: Illustration of the Casson fluid flow schematic

The current problem's modified Navier-Stokes equation is given as:

$$\frac{\partial u}{\partial x}+\frac{\partial v}{\partial y}=0 \quad (5)$$

$$u\frac{\partial u}{\partial x}+v\frac{\partial u}{\partial y}=\nu_{nf}\left(1+\frac{1}{\Lambda}\right)\frac{\partial^2 u}{\partial y^2}-\left(B_0^2\frac{\sigma_{nf}}{\rho_{nf}}\sin^2(\tau)+\frac{\nu_{nf}}{K}\right)u \quad (6)$$

$$\left(\rho c_p\right)_{nf}\left(\frac{\partial T}{\partial t}+u\frac{\partial T}{\partial x}+v\frac{\partial T}{\partial y}\right)=-\left(\nabla\vec{q}+\frac{\partial q_{rad}}{\partial y}\right) \quad (7)$$

here, Λ indicates the Casson fluid parameter, K indicates permeability, $(\nabla\vec{q}+q_{rad})$ is the heat flux.

The boundary conditions are:

$$u=u_w=ax,\ \ v=0,\ \ T=T_w,\ \ at\ \ y=0$$
$$u\to 0,\ \ T\to T_\infty\ \ at\ \ y\to\infty \quad (8)$$

Here u_w is the linear velocity, a is a positive constant, T_w and T_∞ are the wall and for field temperature.

The appropriate transformation of similarity:

$$u=ax\frac{\partial f}{\partial \eta},\ \ v=-\sqrt{a\nu}f(\eta),\ \ \theta(\eta)=\frac{T-T_\infty}{T_w-T_\infty},\ \ \eta=y\sqrt{\frac{a}{\nu}} \quad (9)$$

The variables used in the equations are defined by the terminology.

Momentum equation:

$$A_2 f'''\left(1+\frac{1}{\Lambda}\right)+A_1\left(f''-f'^2\right)-\left(A_3 M\sin^2(\tau)+\frac{A_2}{D_a}\right)f'=0 \quad (10)$$

The appropriate threshold condition decreases to:

$$f'(0)=1\,,f(0)=0\,,f'(\infty)\to 0 \quad (11)$$

Energy equation:

Equation obtained from the Cattaneo-Christov model is as follows:

$$q+\lambda\left[\frac{\partial q}{\partial t}+V.(\nabla q)+(\nabla.V)q-q.(\nabla V)\right]=-k_{nf}\nabla T \quad (12)$$

It is possible to calculate the term K by applying Rosseland's approximation.

$$q_{rad}=-\left(\frac{4\sigma^*}{3k_{nf}^*}\right)\frac{\partial T^4}{\partial y} \quad (13)$$

Where $\sigma^*$is the Stefan–Boltzmann constant and k_{nf}^* is the mean absorption coefficient of the nanofluid. Moreover, we suppose that the temperature difference within the flow is such that T^4 may be expanded in a Taylor series. Hence, expanding T^4 about T_∞ and ignoring higher order terms we get:

$$T^4=4T_\infty^3T-3T_\infty^4 \quad (14)$$

The solution of the equations takes on the following form of an ordinary differential equation upon substitution of the similarity variables defined in Eq. (9) into Eq. (15).

$$\left(u\frac{\partial T}{\partial x}+v\frac{\partial T}{\partial y}\right)+\lambda\left(u\frac{\partial u}{\partial x}\frac{\partial T}{\partial x}+u^2\frac{\partial^2 T}{\partial x^2}+u\frac{\partial v}{\partial x}\frac{\partial T}{\partial y}+v\frac{\partial u}{\partial y}\frac{\partial T}{\partial x}+v\frac{\partial v}{\partial y}\frac{\partial T}{\partial y}+v^2\frac{\partial^2 T}{\partial y^2}+2uv\frac{\partial^2 T}{\partial y\partial x}\right)=\frac{k_{nf}}{\left(\rho c_p\right)_{nf}}\frac{\partial^2 T}{\partial x^2}-\frac{1}{\left(\rho c_p\right)_{nf}}\frac{16\sigma^* T_\infty^3}{3k_{nf}^*}\frac{\partial^2 T}{\partial y^2} \quad (15)$$

$$\frac{1}{A_2}(A_5+R)\theta''+Prf\theta' - Pr\gamma(ff'\theta'+f^2\theta'')=0 \quad (16)$$

Where $D_a=\frac{\rho K a}{\mu}$ is the Darcy number,
$Mn=\frac{\sigma_f}{\rho_f\, a}B_0^2$ is the magnetic parameter,
$P_r=\frac{\mu_f c_{p_f}}{k_f}$ is the Prandtl number, $\gamma=a\lambda$ is the thermal relaxation parameter, $R=\frac{k^*_{nf}k_{nf}}{4\sigma^* T_\infty^3}$ is the radiation parameter.

The energy equation's boundary conditions were reduced to:

$$\theta(0)=1\,,\theta(\infty)=0 \quad (17)$$

The amounts of nanofluid utilized in the findings might be described as:
Here ρ_{nf} is the effective density of the nanofluid, μ_{nf} is the effective dynamic viscosity of the nanofluid, $(\rho c_p)_{nf}$ is the heat capacite of the nanofluid and k_{nf} is the thermal conductivity of the nanofluid are given as:

$$\rho_{nf} = (1-\phi)\rho_f + \phi\rho_p$$
$$(\rho Cp)_{nf} = (1-\phi)(\rho Cp)_f + \phi(\rho Cp)_p$$
$$\mu_{nf}=\frac{\mu_f}{(1-\phi)^{2.5}} \quad (18)$$
$$K_{nf}=\left[\frac{K_s+2K_f-2\phi(K_f-K_s)}{K_s+2K_f+2\phi(K_f-K_s)}\right]K_f$$

Here A_1, A_2, A_3, A_4 and A_5 are dimensionless constants given by:

$$A_1=\frac{\rho_{nf}}{\rho_f}\ ,A_2=\frac{\mu_{nf}}{\mu_f}\ ,A_3=\frac{\sigma_{nf}}{\sigma_f}\ ,$$
$$A_4=\frac{k_{nf}}{k_f},A_5=\frac{(\rho Cp)_{nf}}{(\rho Cp)_f} \quad (19)$$

3 Akbari–Ganji's Method Basic Idea of (AGM)

To comprehend the given method in this paper, the entire process has been declared clearly.

In accordance with the boundary conditions, the general manner of a differential equation is as follows:

$$p_k: f\left(u,u',u'',\dots,u^{(m)}\right)=0;\quad u=u(x) \quad (20)$$

The nonlinear differential equation of p, which is a function of u, the parameter u which is a function of x, and their derivatives are considered as follows: Boundary conditions:

$$\begin{cases} u(x)=u_0,u'(x)=u_1,\dots,u^{(m-1)}(x)=u_{m-1}\ \ at\ \ x=0 \\ u(x)=u_{L_0},u'(x)=u_{L_1},\dots,u^{(m-1)}(x)=u_{L_{m-1}}\ t\ =L \end{cases} \quad (21)$$

To solve the first differential equation concerning the boundary conditions in $x=L$ in Eq. (21), the series of letters in the nth order with constant coefficients which we assume as the solution of the first differential equation is considered as follows:

$$u(x)=\sum_{i=0}^{n}a_ix^i = a_0+a_1x^1+a_2x^2 + a_3x^3 \dots + a_nx^n \quad (22)$$

The more choice of series sentences from Eq. (22) causes a more precise solution for Eq. (20). For obtaining solution of differential Eq. (20) regarding the series from degree (n), there are (n + 1) unknown coefficients that need (n + 1) equations to be specified. The boundary conditions of Eq. (21) are used to solve a set of equations that consists of (n + 1) ones.

Applying the boundary conditions
The application of the boundary conditions for the answer of differential Eq. (21) is in the form of:
When $x\ =\ 0$:

$$\begin{cases} u(0)=a_0=u_0 \\ u'(0)=a_1=u_1 \\ u''(0)=a_2=u_2 \end{cases} \quad (23)$$

And when $x\ =\ L$:

$$\begin{cases} u(L)=a_0+a_1L+a_2L^2+\cdots+a_nL^n=u_{L_0} \\ u'(L)=a_1+2a_2L+3a_3L^2+\cdots+na_nL^{n-1}=u_{L_1} \\ u''(L)=2a_2+6a_3L+12a_4L^2+\cdots+n(n-1)a_nL^{n-2}=u_{L_2} \end{cases} \quad (24)$$

After substituting Eq. (23) into Eq. (20), the application of the boundary conditions on differential Eq. (20) is done according to the following procedure:

$$p_0: f\left(u(0),u'(0),u''(0),\dots\dots,u^{(m)}(0)\right)$$
$$p_1: f\left(u(L),u'(L),u''(L),\dots\dots,u^{(m)}(L)\right) \quad (25)$$

Regarding the choice of n, $(n<\ m)$ sentences from Eq. (21) and to make a set of equations which is consisted of (n+ 1) equations and (n +1); unknowns, we confront with several additional unknowns which are indeed the same coefficients of Eq. (21). Therefore, to remove this problem, we should derive m times from Eq. (20) according to the additional unknowns in the afore-mentioned sets of differential equations and then apply the boundary conditions on them.

$$p'_k : f\left(u', u'', u''', \dots\dots, u^{(m+1)}\right) \quad p''_k : f\left(u'', u''', u^{(IV)}, \dots\dots, u^{(m+2)}\right) \tag{26}$$

Application of the boundary conditions on the derivatives of the differential equation Pk in Eq. (75) is done in the form of:

$$P'_k : \begin{cases} f\left(u'(0), u''(0), u'''(0), \dots\dots, u^{(m+1)}(0)\right) \\ f\left(u'(L), u''(l), u'''(L), \dots\dots, u^{(m+1)}(L)\right) \end{cases} \tag{27}$$

$$P''_k : \begin{cases} f\left(u''(0), u'''(0), u^{(IV)}(0) \dots\dots, u^{(m+2)}(0)\right) \\ f\left(u''(L), u'''(L), u^{(IV)}(L) \dots\dots, u^{(m+1)}(L)\right) \end{cases} \tag{28}$$

(n+ 1) equations can be made from Eq. (22) to Eq. (27) so that (n + 1) unknown coefficients of Eq. (21) such as a_0, a_1, $a_2 . . . . a_n$. Be computer. The solution of the nonlinear differential Eq. (20) will be gained by determining coefficients of Eq. (21). To comprehend the procedures of applying the following explanation we have presented the relevant process step by step in the following part.

Application of Akbari–Ganji's Method (AGM)

According to the mentioned coupled system of nonlinear differential equations and by considering the basic idea of the method, we rewrite Eqs. (10) – (16) in the following order:

$$F(\eta) = A_2 f'''\left(1 + \frac{1}{\Lambda}\right) + A_1\left(f'' - f'^2\right) - \left(A_3 M \sin^2(\tau) + \frac{A_2}{D_a}\right) f' = 0 \tag{29}$$

$$G(\eta) = \frac{1}{A_2}(A_5 + R)\theta'' + Prf\theta' - Pr\gamma\left(ff'\theta' + f^2\theta''\right) = 0 \tag{30}$$

Due to the basic idea of AGM, we have utilized a proper trial function as solution of the considered differential equation which is a finite series of polynomials with constant coefficients, as follows:

$$f(\eta) = \sum_{i=0}^{9} a_i \eta^i = a_0 + a_1\eta^1 + a_2\eta^2 + a_3\eta^3 + a_4 x^4 + a_5 x^5 + a_6 x^6 + a_7 x^7 + a_8 x^8 + a_9 x^9 \tag{31}$$

$$\Theta(\eta) = \sum_{i=0}^{9} b_i \eta^i = b_0 + b_1\eta^1 + b_2\eta^2 + b_3\eta^3 + b_4 x^4 + b_5 x^5 + b_6 x^6 + b_7 x^7 + b_8 x^8 + b_9 x^9 \tag{32}$$

4 Validation of Numerical Results and Discussion of Results

In this work, the steady MHD nanofluid flow and heat transfer past a porous stretching sheetin the attendance of thermal radiation impacts and considering the Christov Cattaneo heat flux model of heat conduction are studied Semian-alytically by using the Akbari Ganji's Method (AGM). To verify the present analytical solution, we compared our results with results given by using Runge-Kutta. They are in excellent agreement as they have been demonstrated in Figure 2.

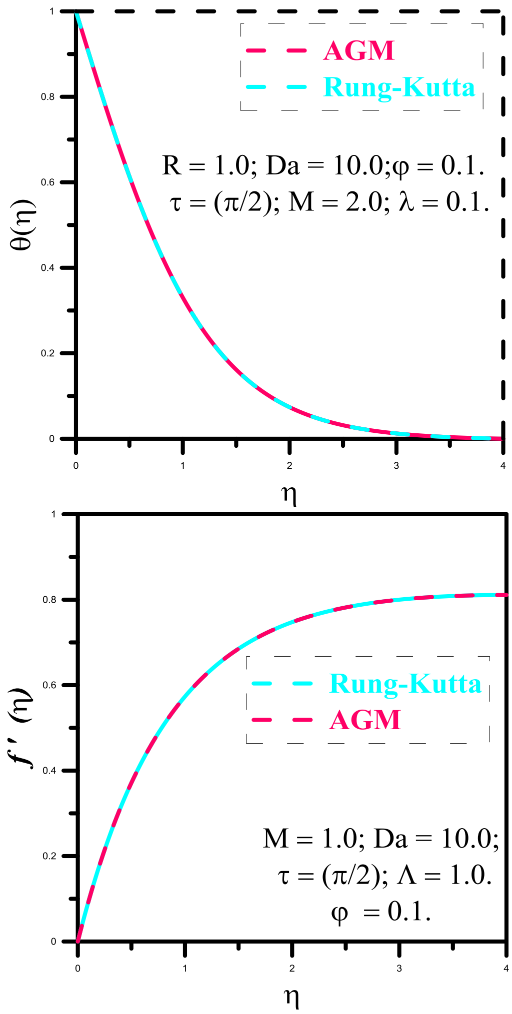

Fig. 2: Comparison between results given by AGM and RK for $f(\eta)$ and $\theta(\eta)$

The current analysis looks at an incompressible Casson fluid flow with MHD and a porous medium. We look into the Silver-Water nanofluid in more detail. The Akbari Gangi Method is then used to solve the ensuing equations that are acquired. The results can be verified using the solid volume fraction, magnetic parameter, radiation parameter, and so on. The current challenge uses a range of physical parameters: $Pr = 6.2$, $\varphi = 0.1$, $\Lambda = 0\ to\ \infty$, with all other parameters modified with suitable values to obtain appropriate parameters. The Cattaneo-Christovs idea, which considered the significance of downtime, serves as the foundation for the current investigation. These changes in thermal conductivity are characteristics that are temperature dependent.

Figure 3 shows the relationship between $f(\eta)$ and η for various M values. In this, when M values rise, $f(\eta)$ values decrease. Figure 4 shows a similar effect of $f(\eta)$ when we change the Λ values, i.e., the $f(\eta)$ lowers as the Λ values increase. Figure 5 illustrates how $f(\eta)$ affects ETA when DA^{-1} values are taken in ascending order. It can be observed that the $f(\eta)$ increases in value with small values of DA^{-1} and declines with increasing DA^{-1} values.

The influence of $f'(\eta)$ vs η for various M values and φ was shown in Figure 6 and Figure 7, respectively. $f'(\eta)$ in Figure 6 has an inverse relationship with M's values. Figure 7 illustrates this same effect, where $f'(\eta)$ decays as φ values rise. Figure 8 illustrates the impact of $f'(\eta)$ vs η for the values of Λ in ascending order. This indicates that $f'(\eta)$ is inversely proportional to Λ, meaning that $f'(\eta)$ is greater for lower Λ values.

The impact of $\theta(\eta)$ versus η for changing the values of R and M, respectively, is shown in Figure 9 and Figure 10. We deduce from Figure 9 that when R values rise, $\theta(\eta)$ also rises. Like this, $\theta(\eta)$ rises as M increases, as shown in Figure 10.

Figure 11 shows the comparison between $\theta(\eta)$ and η for different φ values. In this case, the $\theta(\eta)$ rises as the φ values do, the same effect is observed in Figure 12 for the the impact of Λ on $\theta(\eta)$.

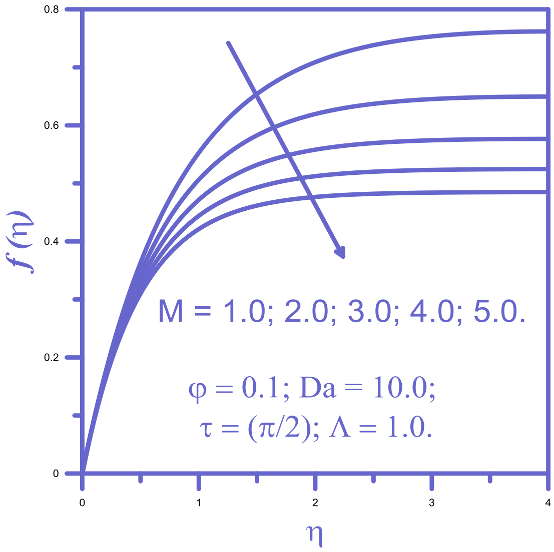

Fig. 3: The impact of M on $f(\eta)$

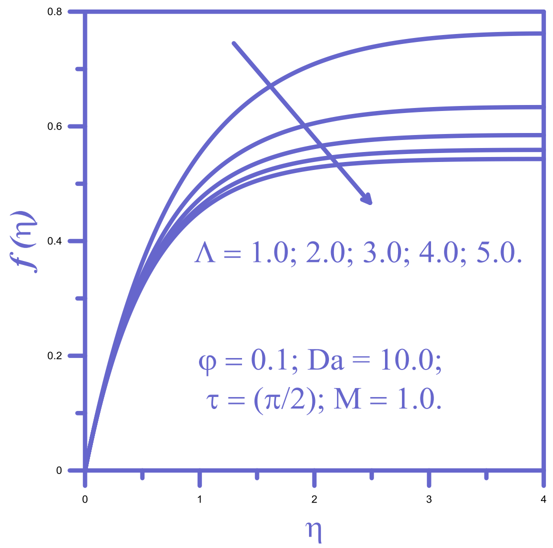

Fig. 4: The impact of Λ on f(η)

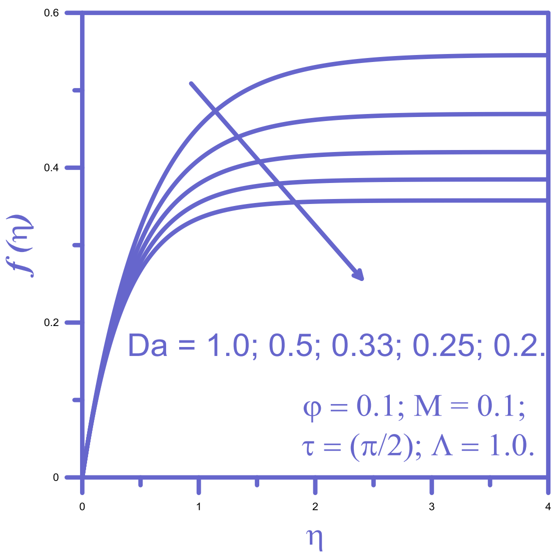

Fig. 5: The impact of Da on f(η)

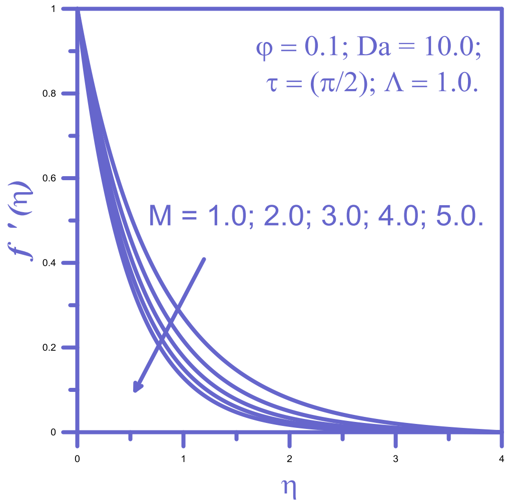

Fig. 6: The impact of M on $f'(\eta)$

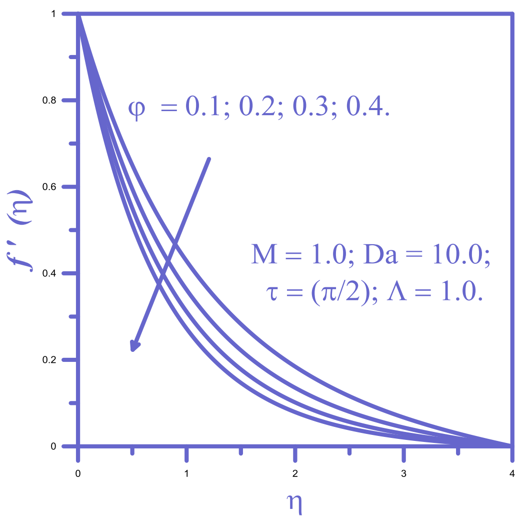

Fig. 7: The impact of φ on $f'(\eta)$

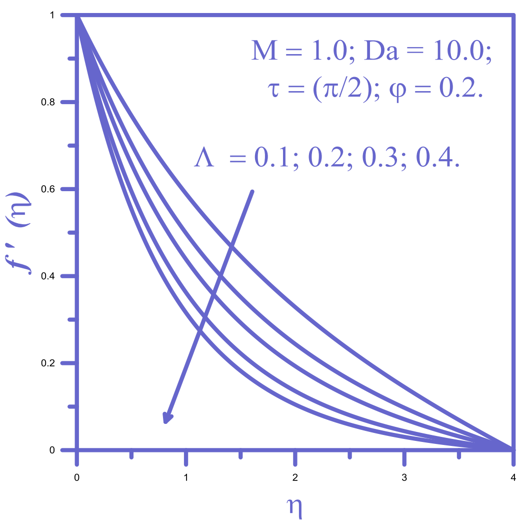

Fig. 8: The impact of Λ on $f'(\eta)$

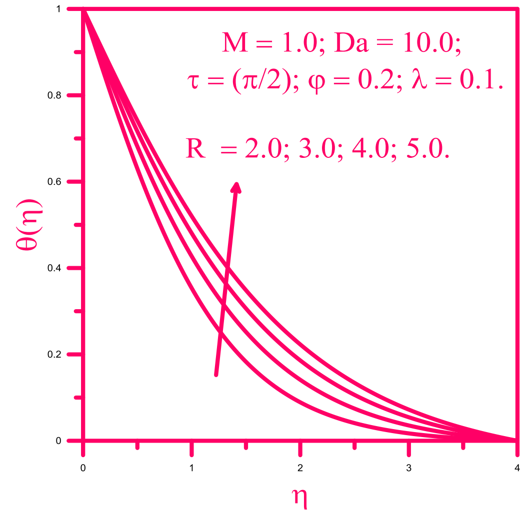

Fig. 9: The impact of R on $\theta(\eta)$

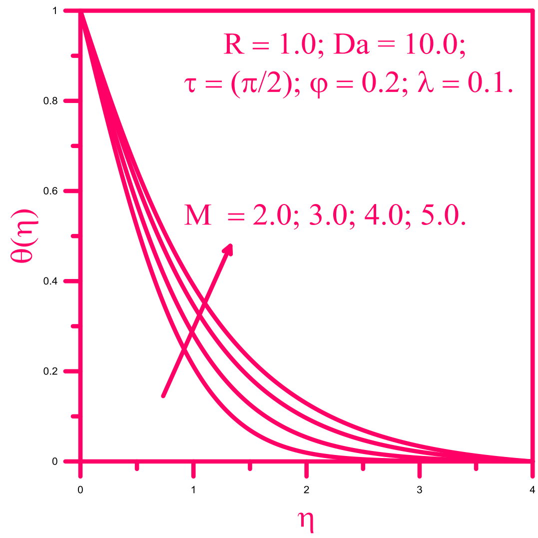

Fig. 10: The impact of M on $\theta(\eta)$

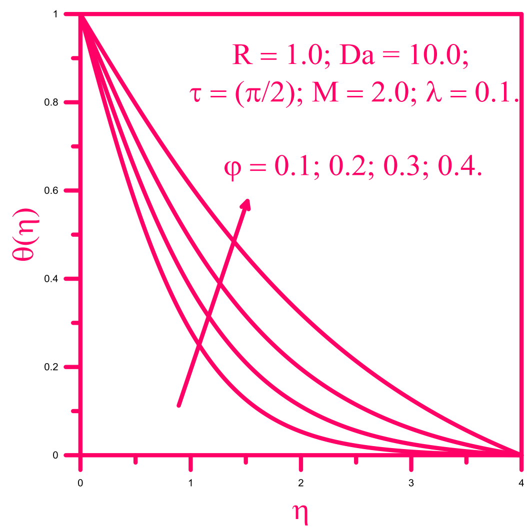

Fig. 11: The impact of φ on $\theta(\eta)$

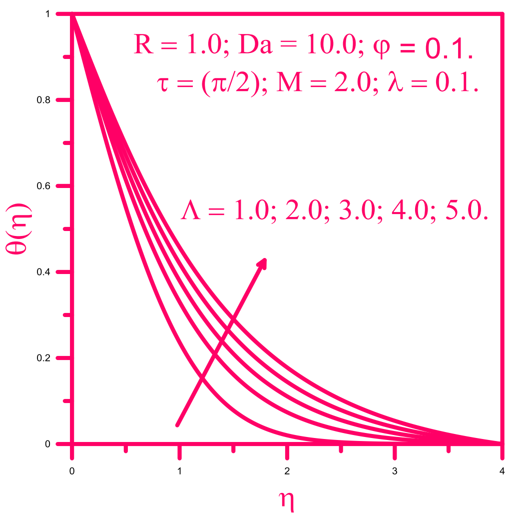

Fig. 12: The impact of Λ on θ(η)

4 Conclusion

The current study investigates the flow of an incompressible, non-Newtonian fluid in the presence of heat radiation, a porous material with an inverse Darcy number, and MHD. Using AGM, the resultant equations are solved analytically. The result is also analyzed using a silver water nanofluid. Using this solution, we get the following conclusions.

- When M is added, the tangential and transverse velocities drop.
- As Λ values increase, $f(\eta)$ also rises.
- φ and $f'(\eta)$ have an inverse relationship.

References:

[1] M.M. Amin, M.H. Ahmadi, M.B. Fatemeh Joda, V. Antonio, S. Uson, Exergy analysis of a Combined Cooling Heating and power system integrated with wind turbine and compressed air energy storage system, *Eng. Conv. Management*. 131 (2017) 69– 78.

[2] B.C. Sakiadis, Boundary layer behaviour on continuous solid surface, *AIchE J.* 7 (1961) 26.

[3] L.J. Crane, Flow past a stretching plate, Zeitschift fur Angewandte *Mathematik and Physik* 21 (1970) 645–647.

[4] U.S. Mahabaleshwar, I.E. Sarris, A.H. Antony, G. Lorenzini, I. Pop, An MHD couple stress fluid due to a perforated sheet undergoing linear stretching with heat transfer, *Int. Jour. Heat Mass Transf.* 105 (2017) 157–167.

[5] U.S. Mahabaleshwar, K.R. Nagaraju, P.N. Vinay Kumar, D. Baleanu, G. Lorenzini, An exact analytical solution of the unsteady magnetohydrodynamics nonlinear dynamics of laminar boundary layer due to an impulsively linear stretching sheet, Continuum mech. *Therm*. 29 (2017) 559–567.

[6] A. Tamayol, K. Hooman, M. Bahrami, Thermal analysis of Flow in a porous medium over a permeable stretching wall, *Transp Porous med* 85 (2010) 661–676.

[7] M. Sharifpur, A.A. Saheed, J.P. Mayer, Experimental investigation and model development for effective viscosity of Al2O3-glycerol nanofluids by using dimensional analysis and GMDH-NN methods, Int. Commun. *Heat Mass Transf.* 68 (2015) 208–219.

[8] M. Sharifpur, S. yousefi, J.P. Meyer. A new model for density of nanofluids including nanolayer. Int. Commun. *Heat Mass Transf.* 78, (2016), 168-174.

[9] M. Sharifpur, N. Tshimanga, J.P. Mayer, O. Manca, Experimental investigation and model development for thermal conductivity alpha- Al2O3-glecerol nanofluids, *Int. Commun. Heat Mass Transf.* 85 (2017) 12–22.

[10] U.S. Mahabaleshwar, P.N. Vinay Kumar, M. Sheremet, Magnetohydrodynamics flow of a nanofluid driven by a stretching/shrinking sheet with suction, *Springer plus.* 5 (2016) 1–9.

[11] L.T. Benos, N.D. Polychronopoulos, U.S. Mahabaleshwar, G. Lorenzini, I.E. Sarris, Thermal and flow investigation of MHD natural convection in a nanofluid saturated porous enclosure: an asymptotic analysis, *J. Therm. Anal. Calorim.* 1–15 (2019).

[12] M. Sharifpur, A.B. Solomon, T.L. Ottermann, J.P. Mayer, Optimum concentration of nanofluids for heat transfer enhancement under cavity flow natural convection with TiO2- water, *Int. Commun. Heat and Mass Transf.* 98 (2018) 297–303.

[13] M. Sharifpur, N. Tshimanga, J.P. Mayer. Parametric analysis of effective thermal conductivity models for nanofluids. *ASME Int. Jour. Mech. Eng. Congress and Exposition.* 45257, (2012), 1-11.

[14] M. Sharifpur, O.G. Solomon, K.Y. Lee, H. Ghodsinezhad, J.P. Mayer, Experimental investigation into natural convection of Zinc Oxide/water nanofluids in a square cavity, *Heat Transf. Eng.* (2020) 1–13.

[15] M.H. Ahmadi, M.A. Nazari, R. Ghasempour, H. Madah, M.B. Shafii, M.A. Ahmadi. Thermal conductivity ratio prediction of Al2O3/water nanofluid by applying connectionist methods. Collides and Surfaces A: Physiochemical and Eng. *Aspects.* 541, 154-164.

[16] C. Cattaneo, *On the conduction of heat, Atti Semin* (Sulla conduzione del calore, Atti Semin), Mat. Fis. Univ. Modena Reggio Emilia. 3 (1948) 83–101.

[17] C.I. Christov, On frame indifferent formulation of the Maxwell- Cattaneo model of finite-speed heat conduction, *Mech. Res. Commun.* 36 (2009) 481–486.

[18] U.S. Mahabaleshwar, M.B. Rekha, P.N. Vinay Kumar, F. Selimefendigil, P.H. Sakanaa, G. Lorenzini, S.N. Ravichandra Nayakar, Mass transfer characteristics of MHD Casson fluid flow past stretching/shrinking sheet, *Jour. Eng. Therm.* Phys. 29 (2020) 285–302.

[19] T. Anusha, Huang-Nan Huang, U.S. Mahabaleshwar. Two-dimensional unsteady stagnation point flow of Casson hybrid nanofluid over a permeable flat surface and heat transfer analysis with radiation. *Jour. Taiwan Inst. Chem. Eng.* (2021).

Contribution of Individual Authors to the Creation of a Scientific Article (Ghostwriting Policy)

A. EL Harfouf: Conceptualization, Formal analysis, Investigation, Methodology, Project administration, Resources, Validation, Writing – original draft, Data curation, Software, Visualization. **R. Herbazi:** Conceptualization, Formal analysis, Investigation, Methodology, Project administration, Resources, Validation, Writing – review & editing. **S. Hayani Mounir:** Conceptualization, Investigation, Project administration, Writing – review & editing. **H. Mes-adi:** Conceptualization, Formal analysis, Investigation, Methodology, Project administration, Resources, Validation, Writing – review & editing. **A. Wakif:** Conceptualization, Investigation, Project administration, Supervision, Writing – review & editing.

Sources of Funding for Research Presented in a Scientific Article or Scientific Article Itself

No funding was received for conducting this study.

Conflict of Interest

The authors have no conflicts of interest to declare.